

## Molecular photovoltaics

Jacques E. Moser, Pierre Bonnôte, Michael Grätzel \*

*Laboratoire de Photonique et Interfaces, Institut de Chimie Physique,  
Ecole Polytechnique Fédérale de Lausanne, CH-1015 Lausanne, Switzerland*

Received 7 July 1997; accepted 19 November 1997

### Contents

Abstract	245
1. Dynamics of charge transfer processes involving molecular sensitizers	245
2. Molecular based photochromic and electrochromic systems	248
References	250

---

### Abstract

Photoinduced charge transfer processes involving molecules adsorbed at interfaces are a fascinating topic which is presently attracting wide attention. Our investigations have focused on the identification of the factors that control the dynamics of such processes. The goal is to design molecular electronic devices that achieve efficient light-induced charge separation. Applications of similar systems in photochromic and electrochromic devices also appear feasible. © 1998 Elsevier Science S.A.

**Keywords:** Solar cells; Nanocrystalline  $\text{TiO}_2$  sensitization; Mesoporous junctions; Photochromic and electrochromic devices

---

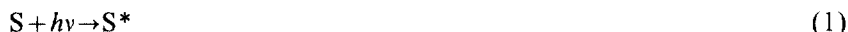
### 1. Dynamics of charge transfer processes involving molecular sensitizers

Photoinduced interfacial charge transfer between a discrete molecular excited state and a continuum of acceptor levels in a solid is the simplest photochemical surface reaction. Besides its fundamental interest, research in this field is strongly motivated by a large number of practical applications. This process is in fact the basis of redox photosensitization of wide bandgap semiconductors and is involved in most of the photographic and xerographic processes, as well as in the photochemical solar energy

---

\* Corresponding author. Fax: +41 21 693 6100; e-mail: michael.graetzel@epfl.ch

conversion [1,2]:



Charge injection [Eq. (2)] competes kinetically with the decay of the sensitizer's excited state. Hence, for dyes that are characterized by emission lifetimes as short as 1 ns, an ultrafast interfacial electron transfer rate is required to provide high injection yields. Back-electron transfer from the conduction band of the solid to the dye's oxidized state  $S^+$  [Eq. (3)] is equally important for photochemical conversion, since its rate controls the efficiency of the overall charge separation [3,4].

Mesoscopic transparent thin films (4–10  $\mu\text{m}$  thick) supported by a glass substrate and colloidal dispersions, both consisting of nanocrystalline particles ( $\sim 20$  nm diameter) of  $\text{TiO}_2$  anatase semiconductor (bandgap  $\approx 3.2$  eV), are employed. These provide substrate material characterized by a very large effective surface area. Dye molecules carrying carboxylic or phosphonic anchoring groups, or a catechol moiety, are grafted onto the acidic surface of titania. A monolayer of the adsorbed molecules on the particles results in optical densities that can easily exceed unity. Upon pulsed laser light excitation, electron injection from adsorbed sensitizer molecules is monitored by fast spectroscopic techniques.

On titanium dioxide, the photoinduced charge injection process that leads to the oxidized dye  $S^+$  takes place on time scales ranging from 100 fs to several microseconds, depending on the sensitizer used (Table 1). Such a variation of eight orders of magnitude can be accounted for by very different values of the electronic coupling element. Frank–Condon factors are expected to play only a negligible role in systems that should be kinetically near optimum in terms of the Marcus theory. In such a case, where the system is coupled to a continuum of acceptor levels and nuclear degrees of freedom are neglected, the rate constant for charge injection is given by

Table 1

Electronic coupling matrix element  $|V|$  calculated from experimental values of the injection rate constant  $k_{\text{inj}}$  measured by ns and fs laser flash photolysis for various sensitizers adsorbed onto colloidal  $\text{TiO}_2$ .  $\tau_f$  and  $\Phi_{\text{inj}}$  are the excited state lifetime and the injection quantum yield, respectively. In the sensitizers column, L stands for the 4,4'-dicarboxy-2,2'-bipyridyl ligand

Sensitizers	$k_{\text{inj}}$ ( $\text{s}^{-1}$ )	$ V $ ( $\text{cm}^{-1}$ )	$\tau_f$ (ns)	$\Phi_{\text{inj}}$	Refs.
$\text{Ru}^{\text{II}}(\text{bpy})_3$	$2 \times 10^5$	0.04	600	0.1	[5]
$\text{Ru}^{\text{II}}\text{L}_3(\text{H}_2\text{O})$	$3 \times 10^7$	0.3	600	0.6	[5]
Eosin-Y	$9 \times 10^8$	2	1	0.4	[6]
$\text{Ru}^{\text{II}}\text{L}_3(\text{EtOH})$	$4 \times 10^{12}$	90	600	1	[7]
Coumarin-343	$5 \times 10^{12}$	100	10	1	[8]
$\text{Ru}^{\text{II}}\text{L}_2(\text{NCS})_2$	$1 \times 10^{13}$	130	50	1	[9,10]
$\text{Ti}_s^{\text{IV}}$ -Alizarin	$> 10^{13}$	$5 \times 10^3$	—	1	—

the golden rule expression:

$$k_{\text{inj}} = (2\pi/\hbar) \cdot |V|^2 \cdot \rho \quad (4)$$

where  $|V|$  is the electron coupling matrix element and  $\rho$  is the density of electronic acceptor states in the conduction band of the semiconductor [8].

Results displayed in Table 1 show that efficient sensitizers have to be designed in a way that the forward electron transfer step is associated with strong electronic coupling between the  $\pi^*$  orbital of the dye molecule's excited state and the empty  $\text{Ti}^{\text{IV}}$ -3d orbital manifold of the semiconductor, which constitutes the acceptor levels in the conduction band of  $\text{TiO}_2$ . This is effectively achieved in directly linking the sensitizer's moiety that carries the lowest  $\pi^*$  orbital to the surface. Another approach, demonstrated by the case of alizarin which forms strongly colored surface complexes on  $\text{TiO}_2$ , consists of exciting directly a ligand-to-metal charge transfer band, where the role of the metal is played by surface  $\text{Ti}^{4+}$  ions.

Observed injection rate constants of the order of  $10^{13} \text{ s}^{-1}$  certainly preclude complete nuclear relaxation of the dye excited state prior to electron transfer, and suggests that the reaction probably proceeds adiabatically [9,10]. Vibrational relaxation of the excited state of  $\text{RuL}_2(\text{NCS})_2$  has indeed been observed to take place within a few picoseconds. The subsequent thermalization and trapping of hot injected electrons is known to be extremely fast and to occur typically with  $k_{\text{th}} \approx 10^{13} \text{ s}^{-1}$  [11]. Reverse electron transfer which would tend to repopulate the excited state of the sensitizer is therefore prevented.

The rate of the electron recapture process which takes place between the conduction band of the solid and the oxidized dye species  $\text{S}^+$  is slower by more than six orders of magnitude compared to charge injection rates of efficient sensitizers (Table 2).

Although very large reaction driving forces should make the system lie deep in the inverted Marcus region, nuclear tunneling effects, due to high frequency vibrational modes implied in the inner sphere reorganization, weaken the role of the Frank–Condon factor [3]. Therefore, electronic coupling is found once more to dictate to a large extent the kinetics of the charge transfer process, which was found indeed to be temperature- and medium-independent [3,4]. Factors likely to be important in controlling the slow rate of charge recombination include delocalization of injected electrons in the conduction band and carrier trapping in remote defects of the solid (Fig. 1).

Table 2

Thermodynamic and kinetic data related to the back-transfer which takes place between conduction band electrons and oxidized dye species adsorbed on the surface

Sensitizers	$-\Delta G$ (eV)	$\log[k_{\text{b}} (\text{s}^{-1})]$	$ V $ ( $\text{cm}^{-1}$ )	Refs.
$\text{Ru}^{\text{II}}\text{L}_2(\text{NCS})_2$	1.75	6.6	22	[4]
Coumarin-343	1.65	6.0	1.7	[3]
$\text{Ti}^{\text{IV}}$ -Alizarin	1.65	6.1	5.6	[3]

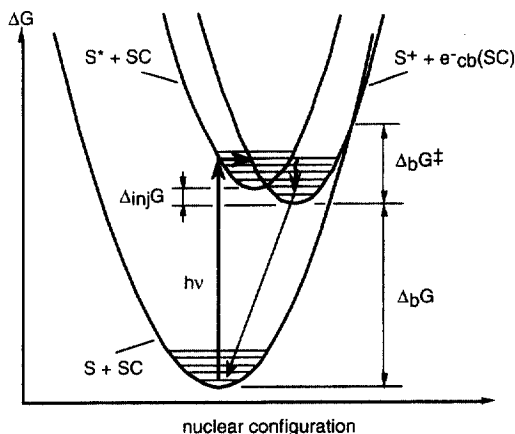
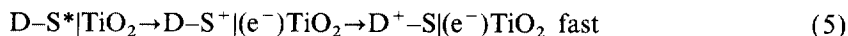


Fig. 1. Conceptual drawing showing free-energy surface crossing for interfacial charge transfer processes depicted by Eqs. (2) and (3). While electron injection is kinetically near optimum ( $\Delta G^\ddagger \approx 0$ ), charge recombination falls deep into the inverted region. In the latter case, nuclear tunneling is likely to occur predominantly, due to efficient contribution of the high frequency vibrational modes and important Frank-Condon overlap.

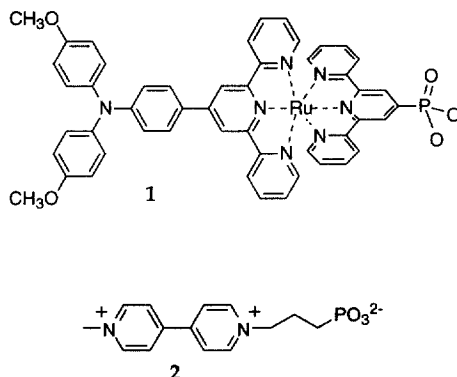
## 2. Molecular based photochromic and electrochromic systems

The linear, rigid molecular diad **1** consisting of an electron donor (triarylamine, D) linked to a chromophore (Ru-bis-terpyridine, S) has been synthesized [12]. The positive redox potentials of **1** are 0.95 V and 1.50 V vs. NHE, respectively assigned to the D/D<sup>+</sup> and the S/S<sup>+</sup> couples. The compound displays an MLCT absorption band at 504 nm ( $\epsilon = 27\,700\text{ M}^{-1}\text{ cm}^{-1}$ ). Electrochemical oxidation to **1**<sup>+</sup> (S–D<sup>+</sup>) is accompanied by blue-shifting of the MLCT band ( $\lambda_{\text{max}} = 488\text{ nm}$ ,  $\epsilon = 22\,500\text{ M}^{-1}\text{ cm}^{-1}$ ) and the development of the absorption band of D<sup>+</sup> at 750 nm, with  $\epsilon = 15\,600\text{ M}^{-1}\text{ cm}^{-1}$ .

When **1** is anchored onto a nanocrystalline TiO<sub>2</sub> film, the heterotriad D–S|TiO<sub>2</sub> produces under illumination a charge-separated state D<sup>+</sup>–S|(e<sup>−</sup>)TiO<sub>2</sub> which decays by charge recombination with  $k = 7 \times 10^7\text{ s}^{-1}$  (70%),  $3 \times 10^5\text{ s}^{-1}$  (20%) and  $4 \times 10^3\text{ s}^{-1}$  (10%) kinetic components.



Photochromism was observed when charge recombination in the heterotriad D–S|TiO<sub>2</sub> is prevented by positive polarization of the supporting conducting glass. At +0.55 V, under illumination with white light, the absorption spectrum of the film changed within a few seconds, with development of an absorption maximum at 750 nm, corresponding to the formation of D<sup>+</sup>–S|TiO<sub>2</sub> (Fig. 2). The initial spectrum (D–S|TiO<sub>2</sub>) was regenerated by applying a potential of −0.3 V. Several



iterations of that cycle were realized without modification of the respective spectra, which opens interesting perspectives towards applications for information storage or smart windows.

Nanocrystalline  $\text{TiO}_2$  films are also a very promising support for the realization of electrochromic devices [13–15]. Exploiting the high surface area of these layers, characterized by a roughness factor reaching 1000 for 10  $\mu\text{m}$  thickness, it was possible to amplify by this factor the change of light absorbance produced by oxidation and reduction of an adsorbed monolayer of electrochromic molecules. Thus, when the potential of a  $\text{TiO}_2$  film modified by a monolayer of an adsorbable viologen like **2** ( $\epsilon = 9000 \text{ M}^{-1} \text{ cm}^{-1}$ ,  $E^\circ = -0.18 \text{ V}$  vs. NHE) was stepped to  $-1 \text{ V}$ , the electrode turned from colorless to deep blue in less than 1 s. The related absorption change at 522 nm was as high as 2. Owing to the position of the conduction band edge of the  $\text{TiO}_2$  (more negative than the redox potential of the viologen), reoxidation of the reduced **2** is not feasible unless protons or lithium ions are added to the electrolyte. In the presence of such potential determining cations, the conduction band edge of  $\text{TiO}_2$  can be lowered to 0 V. Under these conditions, grafted viologens like **2** exhibit reversible electrochemistry. Electrochromic windows up to

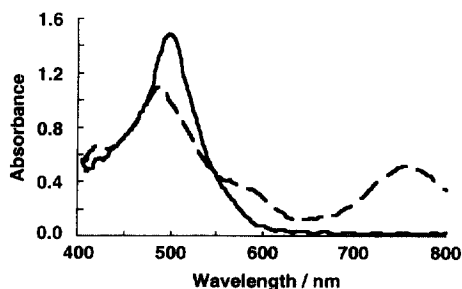


Fig. 2. Absorption spectra of the  $\text{TiO}_2$ -supported diad **1** in the dark (dotted line) and under white light illumination (solid line). The electrode was polarized in both cases at  $+0.55 \text{ V/NHE}$ .

10 cm × 10 cm and small displays were built, using a counterelectrode made of Prussian blue on conducting glass. Very sharp color changes are achieved in 0.5 to 3 s.

## References

- [1] A. Hagfeldt, M. Grätzel, *Chem. Rev.* 95 (1995) 49.
- [2] B. O'Regan, M. Grätzel, *Nature* 353 (1991) 737.
- [3] J.E. Moser, M. Grätzel, *Chem. Phys.* 176 (1993) 493.
- [4] J.E. Moser, *Solar Energy Mater. Solar Cells* 38 (1995) 343.
- [5] J. Desilvestro, M. Grätzel, L. Kavan, J.E. Moser, J. Augustynski, *J. Am. Chem. Soc.* 107 (1985) 2988.
- [6] J.E. Moser, M. Grätzel, *J. Am. Chem. Soc.* 106 (1984) 6557.
- [7] R. Eichberger, F. Willig, *Chem. Phys.* 141 (1990) 159.
- [8] J.M. Rehm, G.L. McLendon, Y. Nagasawa, K. Yoshihara, J.E. Moser, M. Grätzel, *J. Phys. Chem.* 100 (1996) 9577.
- [9] J.E. Moser, M. Grätzel, J.R. Durrant, D.R. Klug, in: M. Chergui (Ed.), *Femtochemistry*, World Scientific, London, 1996.
- [10] J.E. Moser, Y. Tachibana, M. Grätzel, D.R. Klug, J.R. Durrant, *J. Phys. Chem.*, in press.
- [11] D.E. Skinner, D.P. Colombo, J.J. Cavaleri, R.M. Bowman, *J. Phys. Chem.* 99 (1995) 7853.
- [12] P. Bonhôte, J.E. Moser, N. Vlachopoulos, L. Walder, S.M. Zakeeruddin, R. Humphry-Baker, P. Péchy, M. Grätzel, *J. Chem. Soc., Chem. Commun.* (1996) 1163.
- [13] A. Hagfeldt, N. Vlachopoulos, S. Gilbert, M. Grätzel, *Proc. SPIE-Int. Soc. Opt. Eng.* XIII 2255 (1994) 297.
- [14] A. Hagfeldt, L. Walder, M. Grätzel, *Proc. SPIE-Int. Soc. Opt. Eng.* XIV 2531 (1995) 60.
- [15] F. Campus, P. Bonhôte, M. Grätzel, S. Heinen, L. Walder, in preparation.